# Particle Filter-Based Degradation Modeling and SOH Prediction for Lithium-Ion Batteries of Autonomous Systems

Donghoon Seo[1], Taegyun Kim[2], Yeonghyeon Mo[3], Jongho Shin[4] and Seungkeun Kim[5,†]

[1,3,5]*Department of Aerospace Engineering, Chungnam National University, Daejeon, South Korea*
*sseo.dh26@o.cnu.ac.kr*
*ymo@o.cnu.ac.kr*
*skim78@cnu.ac.kr*

[2,5]*Department of Research and Development, Unlabel Inc., South Korea*
*ktg92@cnu.ac.kr*
*skim78@cnu.ac.kr*

[4]*Department of Mechanical Engineering, Chungbuk National University, Cheongju, South Korea*
*jshin@cbnu.ac.kr*

## ABSTRACT

Lithium-ion batteries are widely used in military systems, logistics equipment, and aviation platforms because of their high energy density and long cycle life. However, performance degradation during repeated charge-discharge cycling reduces available capacity and power capability, thereby degrading operational reliability. Accordingly, methods that predict future battery states and estimate the Remaining Useful Life (RUL) from historical degradation behavior are essential for maintenance planning and reliable operation. In this paper, we propose a Particle Filter (PF)-based degradation modeling framework to predict future State of Health (SOH) trajectories and estimate RUL from historical SOH measurements. Battery degradation is represented by a linear combination of time-dependent basis functions, and the corresponding coefficients are treated as latent states to be estimated. Using the observed SOH history as measurements, the PF iteratively estimates the coefficient posterior through particle initialization, state propagation with process noise, weight update, and resampling. The estimated coefficients are then propagated over a future prediction window to generate the SOH trajectory. At the same time, the predictive distribution and prediction interval (PI) are obtained from the particle posterior.

Experimental results show that the proposed method produces stable degradation trajectories while mitigating fluctuations in local observation. In long-horizon extrapolation, predictive uncertainty increases as the particle posterior is propagated through future basis functions. In particular, the trend-related basis terms, $\sqrt{t}$ and $t$, were found to strongly affect both the shape of the mean prediction trajectory and the expansion of the prediction interval. These results indicate that battery degradation prediction should be interpreted not merely as a point-prediction problem but as a distribution-estimation problem that must jointly account for limited historical information and uncertainty in future degradation trends.



† Corresponding Author, E-mail: skim78@cnu.ac.kr

## 1. Introduction

Lithium-ion batteries are increasingly used as a primary energy source in unmanned vehicles, military systems, logistics automation equipment, and aviation platforms because of their high energy density and long cycle life. However, battery degradation is inevitable owing to repeated charge-discharge cycling, variations in operating conditions, and the cumulative effects of internal electrochemical reactions. Such degradation leads not only to capacity fade but also to changes in output characteristics and reduced operational reliability. Therefore, technologies that can quantitatively diagnose battery condition and predict future degradation behavior are of considerable importance (Lu et al, 2023).

A variety of approaches have been studied for battery prognostics, including empirical degradation models, data-driven regression models, and probabilistic state estimation methods. Empirical models are easy to interpret, but their reliance on fixed functional forms may limit adaptability to changing degradation patterns and can result in large extrapolation errors over long prediction horizons (Oji et al, 2021). Data-driven models can learn highly nonlinear relationships, but they often require large amounts of data and may not provide uncertainty information in an interpretable manner. (Zhang et al, 2023). Particle filters (PFs) provide a useful compromise between these approaches, because they retain a relatively simple degradation model while simultaneously estimating the parameter posterior and the predictive distribution.

In this study, we propose a PF-based degradation prediction method to forecast future State-of-Health (SOH) trajectories and estimate remaining useful life (RUL) from historical SOH measurements. The proposed method estimates the coefficients of a degradation model composed of time-dependent basis functions and extrapolates the resulting model over a future prediction window. In addition, the initial parameter distribution is determined using only the currently available input window, thereby reflecting a realistic prediction scenario in which future information is unavailable. By constructing prediction intervals from the particle posterior, the method also enables interpretation of uncertainty long-horizon prediction under limited historical information. Finally, through an analysis of the extrapolated trajectories, we examine how the $\sqrt{t}$ and $t$ basis terms influence both the mean degradation profile and the growth of predictive uncertainty.

## 2. Problem Formulation and Methodology

### 2.1 Problem Formulation

The objective of battery SOH prediction is to forecast the future SOH trajectory from the observed SOH history and to estimate the RUL until a predefined critical SOH threshold is reached. In this study, we consider the problem of predicting the SOH sequence over a prediction window of length $N_p$ using the SOH history over a usage window of length $N_u$ as input.

Because the prediction target lies in an unobserved future window, extrapolation is considered rather than interpolation within an already observed interval. Therefore, it is necessary to consider not only the goodness-of-fit over the usage window but also the uncertainty associated with future prediction.

Therefore, this study addresses the problem of predicting $y_p$ from $y_u$, where the observed SOH of the usage window is $y_u = [y_1, y_2, y_3, ..., y_{N_u}]^T$, and the predicted SOH of the future window is $y_p = [y_{N_u+1}, y_{N_u+2}, y_{N_u+3}, ..., y_{N_u+N_p}]^T$.

### 2.2 Particle Filter Design

#### 2.2.1 Degradation Model

Battery degradation is modeled as a linear combination of time-dependent basis functions. The predicted SOH at time $t$ is defined as follows:

$$\hat{y}(t) = b + \sum_{k=1}^{4} \theta_k \phi_k(t) \quad (1)$$

where $b$ denotes the bias term, $\theta_k$ denotes the coefficient of the $k$-th basis function, and $\phi_k(t)$ denotes the corresponding time-dependent basis function. t is the cycle index defined based on the battery usage history. Specifically, in the usage interval, $t$ is defined as $t$ = 1, 2, ..., $N_u$, and in the prediction interval, the same criteria are maintained, extending $t$ to $t$= $N_u$+1, ..., $N_u$+$N_p$. Therefore, the basis functions in this study represent the patterns of SOH changes that occur as charge-discharge or operational cycles accumulate, rather than the passage of time itself. In this study, four basis functions are used: $sin(t)$, $cos(t)$, $\sqrt{t}$ and $t$. The sine and cosine terms are employed to capture, at a lower dimension, the short-term fluctuations caused by local variations, recovery fluctuations, and measurement noise in the raw SOH measurements or estimated SOH values. In contrast, the √t and t terms serve as trend terms to represent the long-term degradation trend and the gradual nonlinear decline resulting from accumulated cycles. In previous studies on battery SOH prediction and data-driven degradation modeling, cycle count, cumulative usage, nonlinear trend terms, statistical features, and empirical functions have also been utilized as key explanatory variables or model components (Oji et al., 2021; Zhang et al., 2023).

The state variable of the PF is defined as the coefficient vector $\theta = [\theta_1, \theta_2, \theta_3, \theta_4]^T$, which specifies the degradation model. Each particle corresponds to one possible set of coefficients, and the PF estimates the posterior distribution of these coefficients so that the predicted SOH within the usage window is consistent with the reference signal.

#### 2.2.2 PF-Based Degradation Modeling

The initial particle distribution is determined using only the current usage window, without carrying over parameter estimates from previous starting points. To initialize the particle set, ridge regression is first performed using the basis matrix $\Phi_{train}$ for the usage window and the corresponding reference signal $y_{ref}$. The resulting solution is used as the initial center $\theta_0$. The initial center is obtained by solving the following optimization problem:

$$\theta_0 = \arg\min_{\theta} \| y_{ref} - (b \cdot I + \Phi_{train}\theta) \|_2^2 + \lambda_{init} \|\theta\|_2^2 \quad (2)$$

where $y_{ref}$ denotes the reference signal in the usage window, $b$ is the bias term, $I$ is a vector with all elements equal to 1, and $\lambda_{init}$ is the regularization coefficient for the initial parameter estimation. Based on the fitting residual and the design matrix, an initial spread is then assigned to each parameter, and particles are sampled around the initial center. This procedure places the initial particle set near the most plausible region of parameter space for the current usage window while still allowing the PF to estimate the surrounding posterior distribution.

During PF iteration, the particles are perturbed by process noise. At each iteration, the discrepancy between the particle-based prediction over the usage window and the reference signal is evaluated to assign a weight to each particle. The weight is computed by jointly considering the fitting error over the usage window and the regularization term on the coefficient vector:

$$w_i \propto exp\left(-\frac{1}{2\sigma_m^2 N_u}\left\|y_{ref}-\hat{y}_u^i\right\|_2^2-\lambda_{reg}\left\|\theta^i\right\|_1\right) \quad (3)$$

where $\hat{y}_u^i$ denotes the usage-window prediction generated by the $i$-th particle, $\sigma_m$ is the measurement error scale, and $\lambda_{reg}$ is the regularization coefficient. After the weights are updated, resampling is performed so that particles that better explain the usage-window data are more likely to be retained. By repeating this procedure, the PF forms a posterior distribution over the degradation-model coefficients that explains the degradation behavior within the usage window.

After the PF iterations are completed, the final particle set is propagated through the basis functions over the future prediction window to generate a future SOH trajectory for each particle. Representative predictions and prediction intervals are then derived from these particle-based trajectories and used to predict future SOH and estimate RUL. The key PF settings used in this study are summarized in Table 1.

Table 1. PF configuration

| Parameter | Value |
|---|---|
| Number of particles | 500 |
| Number of PF iterations | 2,000 |
| Process noise scale | 0.05 |
| Initial ridge regularization $\lambda_{init}$ | 0.001 |
| Coefficient regularization $\lambda_{reg}$ | 1.2 |

$\lambda_{init}$ was set to a small regularization value to mitigate the condition number of the basis matrix and overfitting on short training intervals when estimating the initial center θ0 using ridge regression. $\lambda_{reg}$ is a value designed to suppress the coefficient vector from becoming excessively large during the weight update step, thereby reducing the likelihood of the prediction trajectory diverging abnormally or the prediction interval expanding unnecessarily in future intervals. The process noise scale was set to maintain particle diversity while preventing the posterior distribution of coefficients formed during the training interval from becoming excessively spread out.

### 2.3 SOH extrapolation

After the PF iteration, the final particle set can be interpreted as posterior samples of the degradation-model coefficients. By substituting the coefficient vector of each particle into the basis matrix for the prediction window, a future SOH trajectory is obtained for each particle. The future prediction for the $i$-th particle is given by:

$$\hat{y}_p^i = b + \Phi_{pred}\theta^i \quad (4)$$

where $\Phi_{pred}$ is the basis matrix for the prediction window and $\theta^i$ is the coefficient vector of the $i$-th particle. Repeating this calculation for all particles yields a set of future SOH trajectories, from which a representative prediction can be constructed. In this study, the representative prediction is defined as the average of the particle-based future predictions.

The predicted future SOH trajectories are also used to estimate RUL with respect to a predefined critical SOH threshold. Specifically, the prediction-based RUL is computed as the time at which the representative prediction reaches the critical threshold. In addition, because the particle set defines a predictive distribution over the future window, the method enables interpretation of not only the future SOH trajectory but also the uncertainty associated with long-horizon extrapolation.

Accordingly, the proposed approach provides both a representative future SOH trajectory and its associated uncertainty range beyond the usage window. It also enables RUL estimation based on the predicted time at which the SOH reaches the critical threshold. Therefore, the proposed method provides not only a point prediction, but also a predictive distribution for future SOH and a corresponding interpretation of RUL.

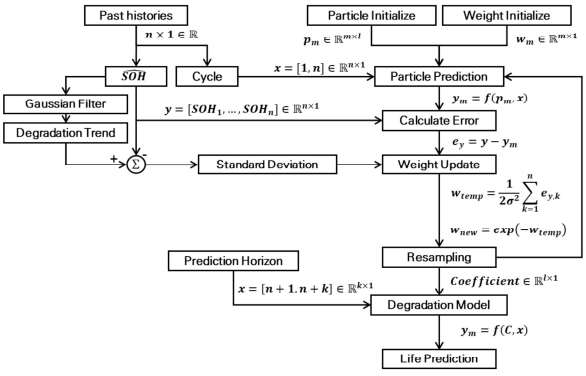


Figure 1. Flow diagram of the proposed method

## 3. Experimental and Evaluation Methods

### 3.1 Experimental Data Configuration

The predictive performance of the proposed method was evaluated using experimental battery discharge data (Seo et al, 2025). The construction procedure for the input SOH data used in this study is described in prior work (Lee et al, 2025). Figure 2 shows the SOH estimation results used to build the input dataset for the present experiments.

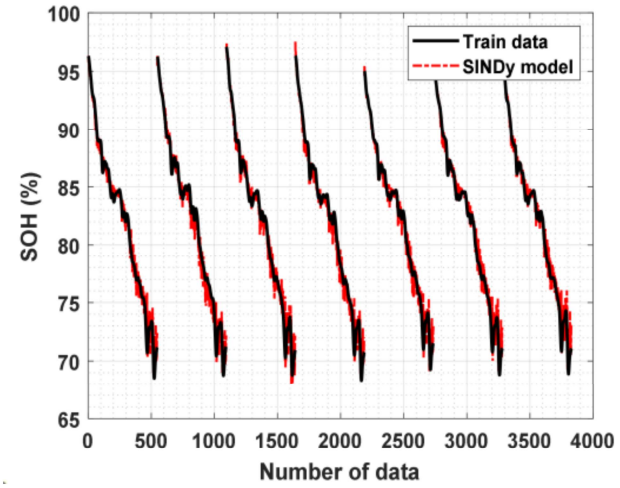


Figure 2. SOH estimation results

For each dataset, the raw SOH measurements were treated as the reference signal, and an additional reference trend was used for fitting the degradation model within the usage window. The prediction experiments were conducted by sequentially defining a usage window and a subsequent prediction window. For each starting point, the SOH history in the usage window was used as input, and the immediately following interval was defined as the target for future prediction. In this study, the length of the usage window was set to $N_u = 50$, and the length of the prediction window was set to $N_p = 50$. In actual operation, the duration represented by the "50-cycle usage range" varies depending on the battery's operating cycle and the frequency of charging and discharging. For example, if one charge-discharge cycle occurs per day, the 50-cycle usage range corresponds to approximately 50 days of operation; under operating conditions involving more frequent charging and discharging, the actual duration may be shorter.

Accordingly, each experiment is structured such that the SOH over the next 50 intervals is predicted from the SOH history observed over the preceding 50 consecutive intervals.

### 3.2 Evaluation Metrics

#### 3.2.1 Numerical Metrics

The proposed method was evaluated in terms of both SOH prediction accuracy and RUL estimation performance over the prediction window. SOH prediction accuracy was quantified by comparing the representative prediction with the reference signal using the root mean square error (RMSE) and the end-of-horizon error (EOE).

RMSE measures the average prediction error over the entire prediction window and is defined as follows:

$$\mathrm{RMSE} = \sqrt{\frac{1}{N_p}\sum_{t=1}^{N_p}\left(\hat{y}(t) - y_{ref}(t)\right)^2} \tag{5}$$

where $\hat{y}(t)$ denotes the representative prediction at time t within the prediction window, and $y_{ref}(t)$ denotes the corresponding reference signal.

EOE measures the prediction error at the final point of the prediction window and is defined as follows:

$$\mathrm{EOE} = \left|\hat{y}(N_p) - y_{ref}(N_p)\right| \tag{6}$$

This metric directly reflects the deviation at the end of the prediction horizon and is therefore useful for assessing the stability of long-horizon extrapolation.

RUL performance was evaluated with respect to a predefined critical SOH threshold. Specifically, the time at which the reference signal reached the threshold was compared with the time predicted by the representative trajectory. This evaluation enabled examination of how the usage-window length, the spread of the particle posterior, and the sensitivity of future extrapolation affected the final RUL estimate.

#### 3.2.2 Prediction Interval, PI

In addition to the representative prediction, this study computes a prediction interval based on the particle posterior. At each time point in the prediction window, the distribution of particle-based predictions is constructed, and the prediction interval is obtained from the quantiles of that distribution. For example, the 90% prediction interval is defined as follows:

$$\mathrm{PI}_{90} = \left[Q_5\left(\hat{y}_p^1,\ldots,\hat{y}_p^N\right), Q_{95}\left(\hat{y}_p^1,\ldots,\hat{y}_p^N\right)\right] \tag{7}$$

where $Q_5$ and $Q_{95}$ denote the 5th and 95th percentiles, respectively. The 95% and 99% prediction intervals can be defined in the same manner. These intervals represent the spread of the particle predictive distribution at each future time point rather than the upper and lower bounds of a single- prediction curve.

To examine how predictive uncertainty evolves with the prediction horizon, the standard deviation of the particle-based predictions is also calculated at each future time point. This quantity indicates how widely the particle posterior

spreads in the output space as the prediction horizon increases. By jointly analyzing the prediction interval and the predictive standard deviation, the present study evaluates not only point-prediction accuracy but also the growth pattern of uncertainty during long-horizon extrapolation.

A comparison of the predictive distributions at the final prediction point showed that the 95% and 99% prediction intervals tended to become excessively wide because they included relatively rare tail particles. For this reason, the 90% prediction interval was adopted as the representative uncertainty band in this study.

## 4. RUL Prediction Results and Analysis

### 4.1 Prediction Results

The prediction results obtained using the proposed method are shown in Figure 3.

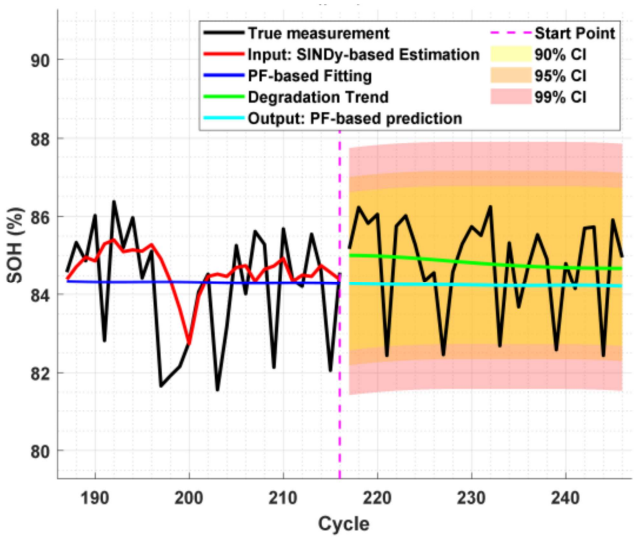


Figure 3. Result of PF-based prediction

Within the usage window, the PF-based method produced a consistent trajectory that reflects the underlying degradation trend in the observed SOH data rather than simply following local fluctuations in the raw measurements. In particular, the method captured the overall decline in SOH while mitigating the effects of local observation noise and transient variations. This behavior can be interpreted as a consequence of forming the particle posterior with respect to the reference trend, thereby prioritizing trajectory consistency over excessive tracking of short-term fluctuations within the usage window.

### 4.2 Uncertainty of Long-Term Prediction

Figure 4 presents prediction results obtained from four different starting points.

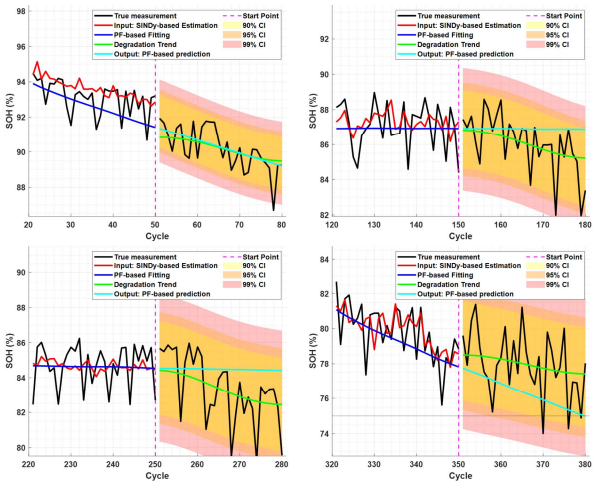


Figure 4. PF-based SOH predictions at four starting points.

In the long-horizon prediction window, future observations are unavailable; therefore, the degradation trend inferred from the observed history may not persist unchanged. This characteristic is reflected in the prediction intervals produced by the proposed method. As shown in Figure 4, an uncertainty band is formed around the representative prediction in the prediction window, and its width generally increases with the prediction horizon. This indicates that the particle posterior spreads more widely in the output space as the forecast extends further into the future.

This phenomenon becomes more pronounced when the available historical data are limited. Under such conditions, predicting degradation behavior beyond the observed interval becomes increasingly difficult, leading to greater predictive uncertainty. The increase in predictive standard deviation over the prediction horizon directly illustrates this effect. In other words, even if multiple particles provide similarly good fits within the usage window, their extrapolated SOH trajectories may diverge substantially in the future prediction window.

These results demonstrate that the proposed PF-based approach not only provides a single-point prediction, but also captures the uncertainty arising from limited historical information and unknown future degradation behavior. This property is particularly important for practical RUL prediction, because long-term battery behavior cannot be observed directly, and degradation patterns may vary depending on the operating conditions. Therefore, from an operational point of view, it is more appropriate to interpret the representative prediction together with the associated prediction interval.

### 4.3 Performance Comparison

To evaluate the effectiveness of the proposed method, we compared it with several empirical degradation models based on fixed functional forms. Each reference model was fitted using only the 50-cycle usage interval and then

extrapolated over the subsequent 50-cycle prediction interval. The reference models used for comparison are defined as follows.

- Case 01: $y = at^3+bt^2+ct+d$
- Case 02: $y = at^2+bt+c$
- Case 03: $y=a \times exp(bt) + ct^2+d$
- Case 04: $y=a \times exp(bt) + ct^2+dt+e$
- Case 05: $y = a \times exp(bt) + c \times exp(dt)$

Here, $t$ denotes the cycle index defined in the usage and prediction intervals, and (a), (b), (c), (d), (e) are the fitting coefficients of each baseline model. Cases 01 and 02 are polynomial-based fixed-function models, while Cases 03–05 are nonlinear fixed-function models that include an exponential term.

Table 2. Comparison of SOH prediction performance

| Metric / Method | RMSE | | EOE | |
|---|---|---|---|---|
| | Min | Max | Min | Max |
| Proposed | **0.0974** | 3.0451 | **0.0017** | **4.1132** |
| Case 01 | 0.5236 | 41.7890 | 0.6978 | 42.4561 |
| Case 02 | 18.4556 | 49.4150 | 34.4867 | 44.4862 |
| Case 03 | 0.1142 | **0.8566** | 0.0116 | 11.4006 |
| Case 04 | 0.1035 | 5.4590 | 0.0148 | 9.8592 |
| Case 05 | 0.1170 | 4.1526 | 0.0085 | 10.4149 |

Table 2 summarizes the SOH prediction performance of the proposed method and the fixed-form baseline models. The proposed PF-based method achieved the lowest minimum RMSE and the lowest EOE values among all compared methods. In terms of the maximum RMSE, Case 03 showed the smallest value; however, the proposed method still maintained relatively low RMSE compared with most fixed-form baselines and achieved the smallest maximum EOE. These results indicate that the proposed method provides more stable end-of-horizon prediction performance when only the 50-cycle usage window is available.

The difference can be attributed to the model structure. The fixed-form baseline models fit a predefined functional form to the usage window and then extrapolate it to the future interval. Therefore, their prediction performance can deteriorate when the future degradation pattern differs from the trend observed in the short usage window. In contrast, the proposed PF-based method estimates multiple possible combinations of degradation-model coefficients in the form of particles and generates a future SOH distribution from them. This allows the method to provide not only a representative prediction but also prediction uncertainty, resulting in more stable SOH prediction under long-horizon extrapolation conditions.

The results also show that predictive uncertainty still increases as the prediction interval becomes longer. This is because future degradation trends cannot be fully determined from a short usage window alone. Therefore, further validation using batteries operated under diverse conditions and longer historical datasets is required to more fully evaluate the generalization performance of the proposed method.

## 5. Conclusion

In this paper, we proposed a PF-based degradation prediction method to forecast future SOH trajectories and estimate remaining useful life from limited historical SOH measurements. The proposed method estimates the coefficients of a time-dependent degradation model using a particle filter, propagates the estimated coefficient posterior over a future prediction window, and simultaneously provides a representative prediction and a prediction interval. In addition, the initial parameter distribution is determined using only the currently available input window , ensuring consistency with a realistic prediction setting.

The experimental results showed that the proposed method generated a stable degradation trajectory within the usage window and provided both a representative future SOH prediction and an uncertainty interval derived from the particle posterior over the prediction window.

At the same time, the results also showed that, because the task is inherently extrapolative, accurately predicting future degradation behavior from limited historical information remains challenging in some cases. This limitation appeared as an expansion of the prediction interval and an increase in prediction error over longer prediction horizons. Nevertheless, compared with an existing empirical degradation model, the proposed method achieved lower prediction error and smaller performance variability, demonstrating greater robustness under limited-history conditions.

Future work will focus on improving the balance between usage-window fitting and extrapolation stability, systematically investigating the effects of regularization and process-noise settings, and performing additional validation under diverse operating conditions and over longer-term datasets. These efforts are expected to further improve the generalization capability and practical applicability of PF-based SOH prediction.

### ACKNOWLEDGEMENT

This research was supported by Unmanned Vehicles Core Technology Research and Development Program through the National Research Foundation of Korea (NRF) and Unmanned Vehicle Advanced Research Center (UVARC) funded by the Ministry of Science and ICT, the Republic of Korea (2020M3C1C1A01083162).

## REFERENCES

Oji, T., Zhou, Y., Ci, S., Kang, F., Chen, X., & Liu, X. (2021). Data-driven methods for battery soh estimation: Survey and a critical analysis. *IEEE Access*, *9*, 126903-126916.

Zhang, M., Yang, D., Du, J., Sun, H., Li, L., Wang, L., & Wang, K. (2023). A review of SOH prediction of Li-ion batteries based on data-driven algorithms. *Energies*, 16(7), 3167.

Lu, J., Xiong, R., Tian, J., Wang, C., & Sun, F. (2023). Deep learning to estimate lithium-ion battery state of health without additional degradation experiments. Nature Communications, 14(1), 2760.

Seo, D., & Shin, J. (2025). State-of-Health (SOH)–Based Diagnosis System for Lithium-Ion Batteries Using DNN With Residual Connection and Statistical Feature. *International Journal of Energy Research*, *2025*(1), 4046189.

Lee, J. D., Seo, D., Shin, J., & Bang, H. (2025). Fast real-time state-of-health estimation method for lithium-ion battery using sparse identification of nonlinear dynamics. *Journal of Intelligent & Robotic Systems*, *111*(3), 93.